



Enhanced Geothermal Systems Creation and Production

Course Number: SU-02-112

PDH: 2

Approved for: AK, AL, AR, GA, IA, IL, IN, KS, KY, LA, MD, ME, MI, MN, MO, MS, MT, NC, ND, NE, NH, NJ, NM, NV, OH, OK, OR, PA, SC, SD, TN, TX, UT, VA, VT, WI, WV, and WY

New Jersey Professional Competency Approval #24GP00025600

North Carolina Approved Sponsor #S-0695

Maryland Approved Provider of Continuing Professional Competency

Indiana Continuing Education Provider #CE21800088

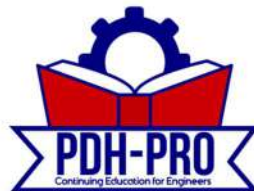
This document is the course text. You may review this material at your leisure before or after you purchase the course. In order to obtain credit for this course, complete the following steps:

1) Log in to My Account and purchase the course. If you don't have an account, go to New User to create an account.

2) After the course has been purchased, review the technical material and then complete the quiz at your convenience.

3) A Certificate of Completion is available once you pass the exam (70% or greater). If a passing grade is not obtained, you may take the quiz as many times as necessary until a passing grade is obtained (up to one year from the purchase date).

If you have any questions or technical difficulties, please call (508) 298-4787 or email us at admin@PDH-Pro.com.



Enhanced Geothermal Systems

Contact: Dan McMorrow — dmcorrow@mitre.org

December 2013

JSR-13-320

Approved for public release; distribution unlimited.

JASON
The MITRE Corporation
7515 Colshire Drive
McLean, Virginia 22102-7508
(703) 983-6997

5 EGS CREATION AND PRODUCTION

5.1 Heat Transfer Features of EGS

Two primary determinants of the possible success of a geothermal system, from conventional hydrothermal to hot dry rock (HDR), are the recovery factors for thermal energy and the possible lifetime of a given producing region. Both features require understanding the coupling of heat transfer to the water and the change of the thermal energy in the rock. These require knowledge of, or models of, the distribution of cracks and associated fluid flow at depth; the latter are poorly constrained, and all models make assumptions about the crack network or the average permeability of the reservoir.

An important characteristic of geothermal energy extraction is that where energy is extracted from a hot rock by contacting the rock with flowing (colder) water, the temperature of the rock is gradually reduced to approach the temperature of the injected water. In the absence of significant permeability of the rock, the thermal recovery of the rock can occur only by heat conduction, which is relatively slow. Hence, heat transfer considerations mean that within $t = 5$ years of contact with cool water the rock has been locally cooled over a distance of $\approx (4\kappa_r t)^{1/2} = (4 \times 5 \text{ yr} \times 30 \text{ m}^2/\text{yr})^{1/2} \approx 25 \text{ m}$ (where κ_r is the thermal diffusivity of the rock). One implication is that if an EGS system is to produce significant useable energy for more than a year or two, it must employ flow strategies that are tailored to the fracture network. In a network of closely spaced fractures, the “cooling waves” from neighboring fractures will quickly meet in the center of the rock that separates them and this rock will no longer push much energy into the water. However, if the flow is sufficiently slow, this will happen first at the injection end of the channels and propagate slowly toward the exit. In a network of widely spaced fractures higher flow speed may be useful, at least until the cooling wave becomes significant at the channel exit. We discuss these considerations, and illustrate them with example calculations, in this section.

There appear to be practical limits to how much energy can be usefully extracted from heat mining efforts once a thermal front has propagated from the injection point to the exit of the heat-transfer region. For example, if a thermal cycle is used to produce electricity, the temperature of the water is just as important as the rate at which energy is extracted from the rock. Below, we describe one strategy for reducing the rate of decay of the produced energy by reducing the water flow rate, which keeps the thermal efficiency reasonably high.

Thermal bypass: In terms of the order of magnitude characterization discussed above (based on thinking about a model set of uniform cracks), we can remark that the temperature of water within cracks wider than b_0 does not approach the far-field rock temperature T_{r0} because it flows too fast for sufficient heat to be conducted through the rock to the flowing water. (The water itself is taken to be isothermal across a narrow crack). Such wide cracks are a source of thermal bypass, mixing their cooler water with hot water from narrower cracks at the production well. Because the typical crack opening b_0 depends on both the pressure gradient and on the time t_r over which geothermal energy has been pumped, this kind of thermal bypass will develop gradually, and may (at the price of reducing the fluid and heat flow rate) be controlled by reducing the pressure gradient (see below). A second class of thermal bypass, resulting from heterogeneous depletion of rock thermal energy (i.e. cooling of the rock), can occur even for cracks narrower than b_0 .

5.1.1 Description of the heat transfer problem

To assess and illustrate the fundamental heat transfer characteristics of an EGS system in HDR, we consider coupled one-dimensional models for temperature evolution in such a system. These models have a long history in geothermal engineering (e.g [82, 83, 84]), and JASON performed similar calculations to make independent assessments of the thermal evolution in the subsurface and to explore tradeoffs available to maximize useful energy

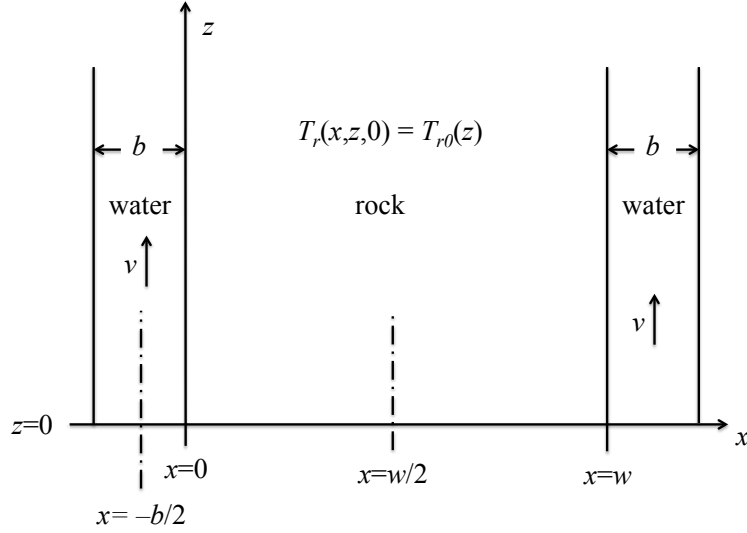


Figure 5-1: A vertical channel of width b and length ℓ (in z) in underground rock, with water injected at temperature T_{w0} flowing upward with speed v . In this section z is vertically upward, consistent with the direction of flow and standard use in heat transfer calculations, but opposite the standard geophysical notation where z is downwards from the Earth's surface.

production. We study first the simple case in which the rock temperature far from the channel remains constant, and we provide quantitative estimates of the time scale on which this is a good approximation. Then we consider later times, for which the rock temperature between flow channels decreases.

The heat transfer from the subsurface is characterized in a straightforward manner *assuming* a crack or simple crack network is present in the rock, e.g. Figure 5-1. Since cracks open up vertically due to the background lithostatic stress we assume for the summary presented here that the fluid flows vertically from an injection well to a production well. The crack opening is expected to be the smallest dimension so a one-dimensional model for the temperature of the water T_w has the form

$$\frac{\partial T_w}{\partial t} + v \frac{\partial T_w}{\partial z} = \kappa_w \frac{\partial^2 T_w}{\partial z^2} + \frac{2j_r}{C_w b}, \quad (5-1)$$

where j_r denotes the heat flux (energy/area/time) transferred from the rock to the water and the factor of 2 accounts for the two surfaces of the crack

(κ_w and C_w are the thermal diffusivity and volumetric specific heat of water, respectively). Typically we expect convective effects to dominate the heat transfer so the conductive term in equation (5-1) is neglected. The thermal evolution in the rock is determined by solving pure heat conduction in the rock:

$$\frac{\partial T_r}{\partial t} = \kappa_r \nabla^2 T_r \quad \Rightarrow \quad \frac{\partial T_r}{\partial t} = \kappa_r \frac{\partial^2 T_r}{\partial x^2}, \quad (5-2)$$

where x is directed into the rock and transverse to the flow direction (see Figure 5-1), with the latter approximation valid since transverse heat conduction occurs on a length scale $(4\kappa_r t)^{1/2} \ll \ell$. The heat flux $j = k_r \frac{\partial T_r}{\partial x}|_{x=0}$ from the rock to the water couples the water and the rock at their common interface, at which it is a good approximation that $T_w = T_r$. This boundary-value problem is well studied in the literature using analytical and numerical methods, e.g. [82], which is the model on which USGS estimates are based [1].

The analysis (see Appendix B) shows that after a time $t_{c1} \propto b^2/\kappa_r$, where b is the channel width, the water temperature in the channel equilibrates with the local rock-surface temperature. This takes only a few minutes for $b \approx 1$ cm. After this brief initial phase and once the first injected water has made its way to the exit of the heat-transfer zone, the equation for the water temperature becomes quasi-steady, i.e. $v \frac{\partial T_w}{\partial z} = \frac{2j_r}{C_w b}$. A “diffusion” front grows into the rock as the water progressively cools the rock, and a “cooling front” propagates from the injection point towards the channel exit. As a result, there is a distinct front between the region in which water has cooled the rock to its injection temperature, a narrow transition region, and a region in which the water has been heated to the initial rock temperature. Most of the heat transfer from rock to water occurs in this transition region.

As mentioned above and discussed in Appendix B, there is a second critical time t_{c2} when the transverse conduction front (“cooling wave”) in the rock has propagated a transverse distance ℓ_T to the mid-point between two parallel cracks. This time is about $t_{c2} \approx \ell_T^2/(4\kappa_r)$. For example, if two parallel cracks are separated by $2\ell_T = 30$ m, the central rock temperature

will decrease on a time scale $t_{c2} \approx 2$ years. Even before this happens, the heat flow to the water has dropped from its initial transfer rate because it is driven by the temperature gradient in the rock, which falls approximately in proportion to $1/t^{1/2}$ if the cooling water temperature at a given position remains constant. Once the cooling waves collide the gradient falls even more quickly.

Finally, there is a third characteristic time scale t_{c3} , which is when the propagating “cooling front” reaches the exit of the heat-transfer zone (on its way to the production well). A balance of terms in the governing equations shows that it should be expected that the water can no longer be heated close to the ambient rock temperature after a time t_{c3} , where

$$t_{c3} \approx \left(\frac{C_r}{C_w} \frac{\ell}{vb} \right)^2 \kappa_r, \quad (5-3)$$

and where C_r and C_w are the volumetric specific heats of rock and water, respectively.

The time scale t_{c1} is short and not important for the performance of the EGS. However, the competition between t_{c2} and t_{c3} has significant implications for the useful energy that can be extracted from an EGS system and for its longevity. We illustrate this with a series of results below, following the discussion of energy production.

5.1.2 Illustrative examples

We illustrate with a series of results, which we obtained by solving our coupled 1D models as detailed in Appendix B. We consider the following geometry:

1. water injection at $z = 0$ at $T_{w0} = 320$ K;
2. heat-exchange distance, ℓ , of 1 km;
3. rock temperature of 550 K at $z = 0$, falling linearly to 525 K at $z = \ell = 1$ km;

4. $b = \text{crack/channel width} = 1 \text{ mm}$;
5. $\Delta y \text{ of channel} = 10 \text{ m}$.

We take typical rock and water material parameters, detailed in Appendix B. We solve for the temperature distribution in the rock and water as a function of time and also compute the electrical power generation as a function of time (see the next section for a description of the calculation of the electrical power generation). We repeat this for different mass flow rates (meaning different flow speeds in this case, since we hold other parameters fixed).

The first example is designed to illustrate how poorly an EGS system can perform if water flows too quickly, which is a concern if there are a few large “bypass” flow channels. A high flow rate extracts the maximum thermal power but does not achieve high water temperatures and thus does not provide much *useful* energy. With the parameters above and a flow speed of 10 m/s, we obtain the results depicted in Figure 5-2. In this and subsequent figures, the color plot on the left illustrates the temperature distribution, with the water channel on the left (shown wider than its real size, for visibility), and the electrical power output is plotted as a function of time on the right. The time of the color plot is the last time at which an electrical power is plotted in the figure. In this first example, the color plot is at 5 years. This example illustrates several points. One is that the cooling wave does indeed propagate $\approx 25 \text{ m}$ into the rock in a time of 5 years. Another is that power output starts low and drops quickly—approximately as $1/t$. We can see from how much the rock has cooled that substantial thermal energy has been mined. However, it has not been very useful, because the water temperature was low, because the flow rate was much faster than optimal. In terms of the critical times t_{c2} and t_{c3} , in this example t_{c3} (the time for the cooling wave to reach the top) is much shorter than t_{c2} (the time for horizontal propagation over a significant distance). This leads to nearly vertical temperature contours in the rock, in contrast to what we will see later.

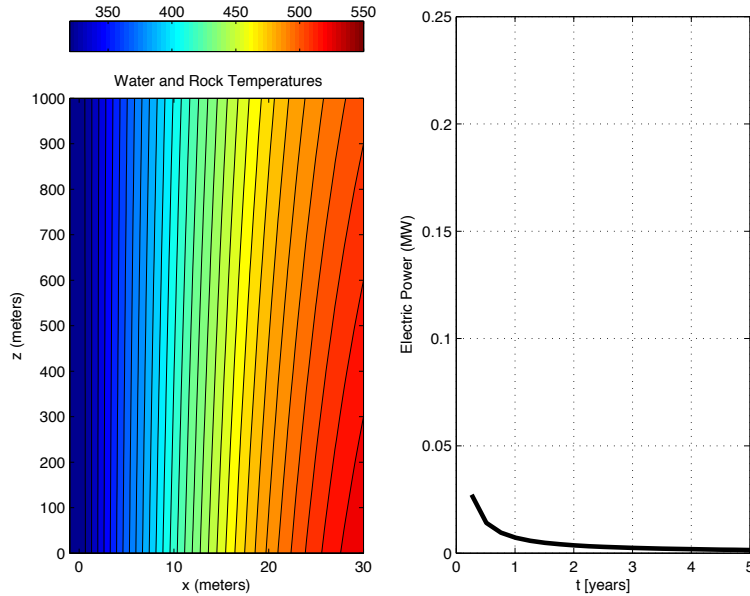


Figure 5-2: Results from example calculation with $v = 10$ m/s, shown at $t = 5$ years. On the left is a color contour plot of temperature in the water and rock system, with the water channel on the left made artificially wide for visibility. On the right is electrical power generation as a function of time. Flow speed is much too fast for useful power generation.

In our second example we reduce the flow by a factor of 10, so that $v = 1$ m/s. Results are shown in Figure 5-3. The rock temperature profile at $t = 5$ years is almost the same as in the $v = 10$ m/s case, which shows that the same amount of energy was mined. Nevertheless, electrical power generation is higher by approximately a factor of 8. This is a significant improvement. However, this is still suboptimal, and power still drops almost as fast as $1/t$.

For the third example we reduce the flow by another factor of 10, so that $v = 0.1$ m/s = 10 cm/s. The state at $t = 5$ years is shown in Figure 5-4. We see qualitative differences between this and the previous cases. Temperature contours in the rock are not vertical, and the water exiting temperature is significantly higher than its entering temperature. Electrical energy generation is substantially higher than in previous cases, and it is not dropping as steeply. The power at early times is only $\approx 20\%$ higher than in the $v = 1$

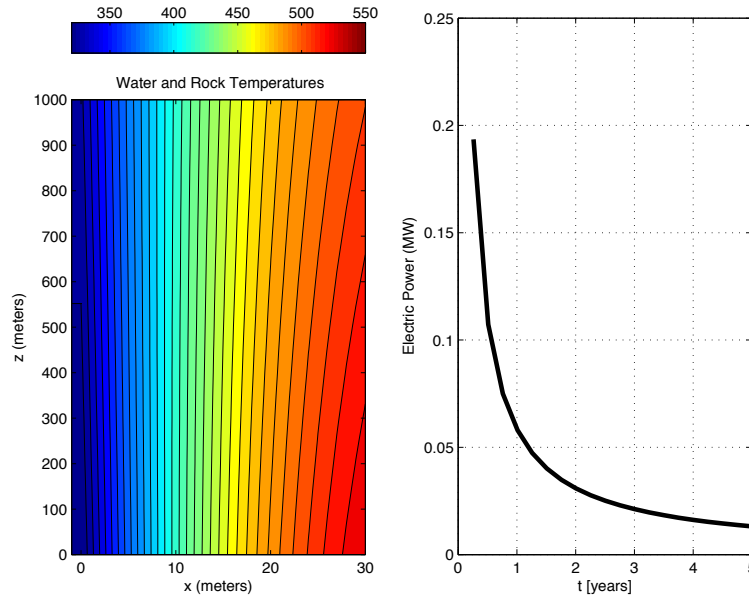


Figure 5-3: Results from example calculation with $v = 1$ m/s, shown at $t = 5$ years. Flow speed is still too fast for optimum power generation, although it is much improved over the $v=10$ m/s case.

m/s case, but at $t = 5$ years it is higher by a factor of ≈ 4 . Comparison of the rock temperature contours at $t = 5$ years shows that with the slower flow speed the system has not mined as much thermal energy, even though it has generated much more electrical energy.

Figure 5-5 shows the temperature field for the same flow speed at an earlier time of $t \approx t_{c3}$, when the rock at the top of the heat-exchange zone has just begun to cool. This illustrates that a flow speed of ≈ 0.1 m/s for this crack geometry makes t_{c2} and t_{c3} approximately the same. We suggest that this is a good guiding principle for maximizing useful energy output, at least until $t \approx t_{c3}$.

The final example illustrates the results of a very slow flow speed. The state at $t = 5$ years is shown in Figure 5-6. Slow flow maximizes water outlet temperature and thus maximizes efficiency of conversion to electricity, but it produces a slow rate of energy extraction. This system would continue

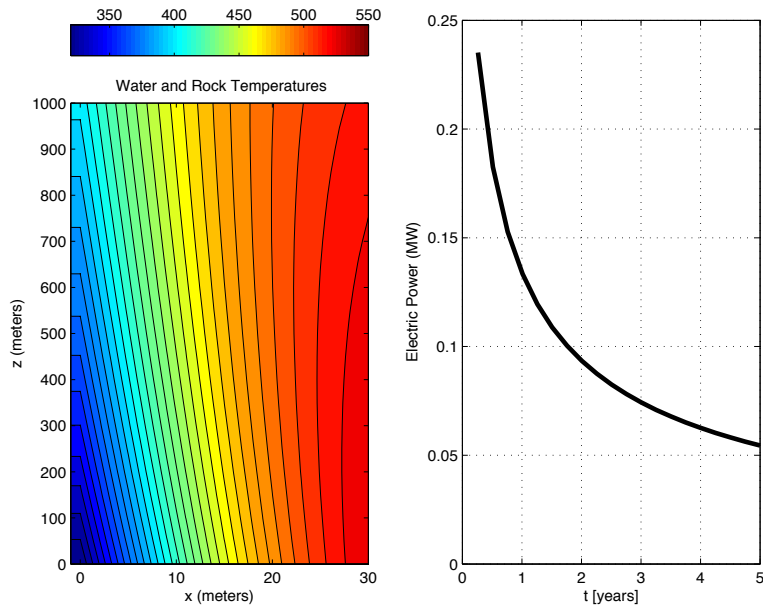


Figure 5-4: Results from example with $v = 0.1$ m/s, shown at $t = 5$ years. This system's performance is substantially improved over the faster-flow systems.

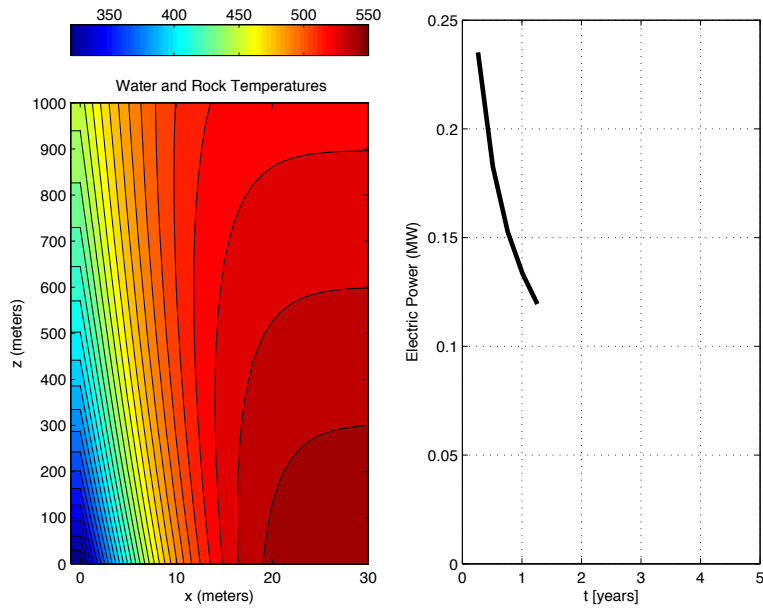


Figure 5-5: Results from example with $v = 0.1$ m/s, shown at $t \approx t_{c3}$.

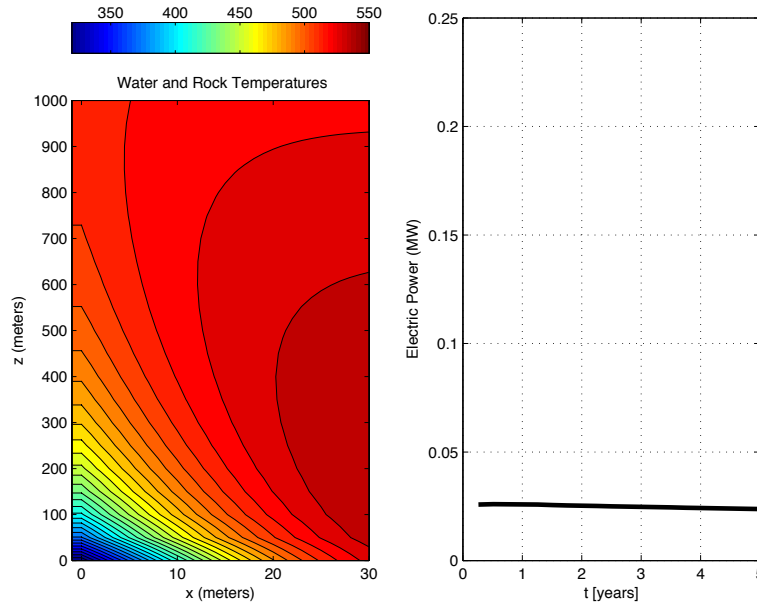


Figure 5-6: Results from example with $v = 0.01$ m/s, shown at $t = 5$ years. Slow flow maximizes water outlet temperature and thus maximizes efficiency of conversion to electricity. It also maximizes the time over which power does not drop substantially from its initial value. The trade-off is that the almost-steady power level is relatively low.

to produce electricity for many years without the substantial drop in output that accompany faster flow systems.

These examples illustrate the crucial role of water flow rate in EGS systems. A network of fractures that has many narrow cracks but a few wider ones will be in danger of performing much like the high-flow examples shown above, with low water outlet temperature and correspondingly low utility of the extracted energy (e.g., abysmal efficiency for electrical generation).

5.1.3 Energy produced as a function of flow rate

An important quantity is the energy transferred to a water channel per unit time (the “thermal” channel power, P_{th}^{ch}). As above, we denote the channel opening b , the mean water speed v , and the injected water temperature

T_{w0} . We can determine the time evolution of the exit temperature $T_{w,ex}$ from a channel of width Δy . We find

$$P_{th}^{ch} = (400 \text{ kW}) \left(\frac{\dot{m}}{1 \text{ kg/s}} \right) \frac{T_w(z_{ex}) - T_{w0}}{100 \text{ K}}, \quad (5-4)$$

where

$$\dot{m} \equiv b \Delta y v \rho_w = \text{mass flow rate.} \quad (5-5)$$

For example, given a 1 mm crack with $\Delta y = 10 \text{ m}$, a flow speed of 10 cm/s corresponds to 1 kg/s of flow. In this case, if the water gains 100 K from the rock during its journey, the 1 mm \times 10 m channel will yield 400 kW of thermal power.

Thermal power is important, but it is not the whole story. We illustrate the importance of exit temperature by considering electricity production. We assume near-maximum thermodynamic efficiency of electricity generation P_e^{ch} in which case the electrical power produced from the heated water is estimated as

$$P_e^{ch} = P_{th}^{ch} \left(\frac{T_{w,ex} - T_{w0}}{T_{w,ex}} \right). \quad (5-6)$$

Combining the previous two equations yields

$$P_e^{ch} = (400 \text{ kW}) \left(\frac{\dot{m}}{1 \text{ kg/s}} \right) \frac{(T_w(z_{ex}) - T_{w0})^2}{(100 \text{ K})T_{w,ex}}. \quad (5-7)$$

This equation highlights the importance of maintaining a high water temperature at the outlet of the heat-exchange zone. EGS flow strategies should be designed with this in mind.

5.1.4 Flow strategies

The examples above considered a variety of flow rates but in each example the flow rate was held constant for the entire five-year period. With some simplifying assumptions we can generalize the behavior of a flow channel under constant flow conditions. We have done this for the channel electrical power as a function of time, and the results are in Figure 5-7.

Given constant flow, we can identify three phases in electrical power production from a given channel: a short phase in which water temperature achieves equilibrium with the rock surface temperature, an intermediate phase as the thermal wave in the rock develops in the z direction, and a final stage in which the electrical power output drops more quickly than it did before t_{c3} . In the final stage, power will eventually drop like $1/t$ even if channels are spaced far apart, and it will drop more quickly if channels are close enough for their cooling waves to interact.

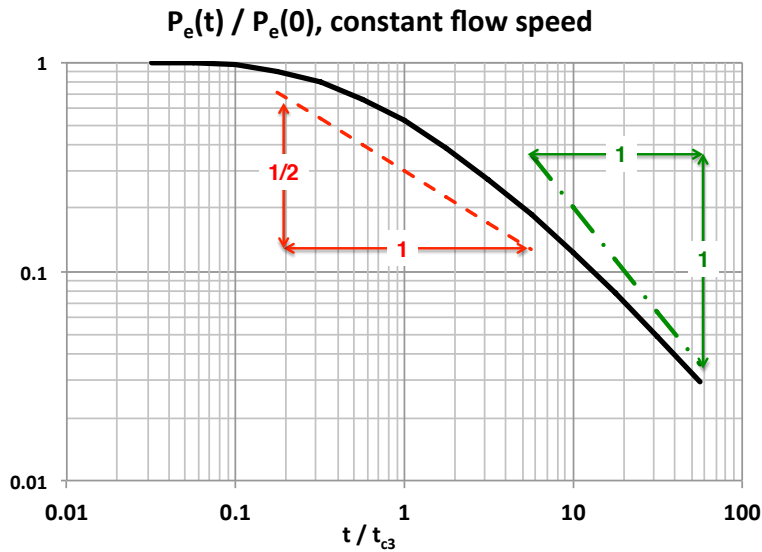


Figure 5-7: Electrical power as a function of time for constant flow conditions during the “intermediate time period. With constant flow conditions there are three phases: an early phase of approximately constant power, a second stage when power drops roughly as $t^{-1/2}$, and a later stage when power drops roughly as t^{-1} .

Figure 5-7 shows a strong decay of power production for times past t_{c3} . We can slow the decay of the power production by altering the flow through the channel. Consider the following flow strategy: begin with constant flow rate until the thermal front in the rock reaches the production well at about t_{c3} , then decrease the water speed in proportion to $t^{-1/2}$. This approach transfers roughly the same amount of energy to the water but keeps the exit temperature constant, and so maintains reasonably high thermal efficiency.

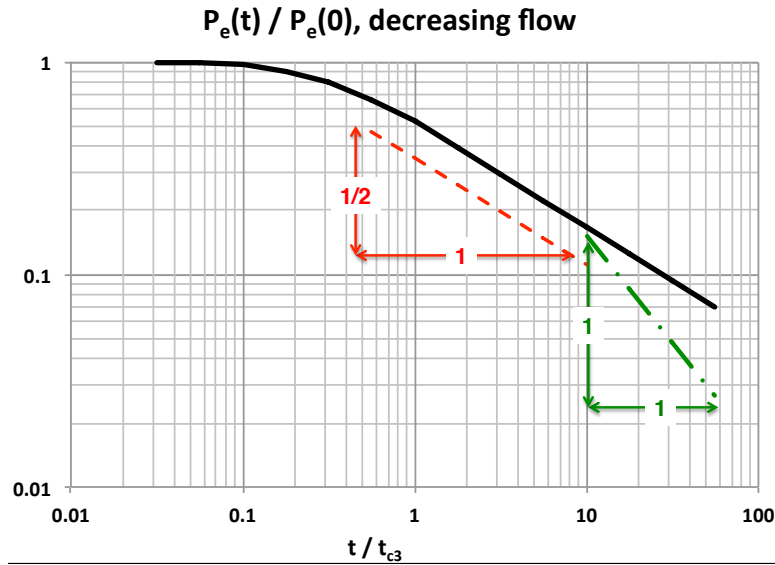


Figure 5-8: Electrical power as a function of time for flow that is constant until the thermal front reaches the production well, after which flow speed drops as $t^{-1/2}$. With this flow strategy, electrical power generated never drops faster than $t^{-1/2}$.

The resulting electrical power production is shown in Figure 5-8. The price for this decrease in flow rate is that the channel thermal power decreases proportional to $t^{-1/2}$. This decrease is not as steep as that of the constant-flow case (Figure 5-7), so this appears to be a superior flow control/heat transfer strategy. Again, for times late enough that the deep-rock temperature decreases because of communication between channels, the power decreases will be steeper than these results indicate. However, this may happen after the power has already dropped enough to end the practical life of the well.

5.1.5 Remarks

The various JASON analyses are consistent with the kinds of hydrodynamic and transport (thermal and chemical) modeling that has been developed in the geothermal field over the past 30+ years, which forms the basis for the quantitative assessments of identified geothermal fields made by the USGS in 2008 [1]. Nevertheless, these assessments assume a fracture field

exists for the flow and heat exchange, and highlight that the spatial features and heterogeneities of the fractures, i.e. the reservoir permeability, is the primary uncertainty in being able to provide rational assessments of the short- and long-term features of geothermal sites. This viewpoint further emphasizes the need for subsurface characterization. It also provides motivation for the JASON suggestion to consider engineering subsurface heat-exchange systems as one route to eliminating uncertainty in the subsurface heat transfer necessary for power production.

5.2 Wholly Drilled Heat Exchanger

Advances in drilling technology and in particular advances in micro drilling suggest that it is worthwhile to consider engineering permeability in otherwise dry rock by drilling properly spaced holes directly between injection and production wells. Various detailed calculations are possible but here we simply estimate the mean power possible if the water can be heated to approximately the mean temperature between the rock and the injected water.

An upper bound on the energy to be produced is to assume that thermal energy is extracted in time t_r from the hot rock over a radial distance $\sqrt{\kappa_r t_r}$. Then, per unit length of such a drilled circular hole we extract energy from the surrounding rock on a volume $\pi (\sqrt{\kappa_r t_r})^2 \ell$, or

$$\text{energy/length in time } t_r = (C_r \Delta T) \pi \kappa_r t_r \quad (5-8)$$

which corresponds to a maximum power (per length of pipe)

$$\text{average power/length} = (C_r \Delta T) \pi \kappa_r. \quad (5-9)$$

Using typical values for rock (granite), and assuming a temperature change $\Delta T = 100^\circ\text{C}$ we find

$$\text{average power/length} \approx 0.75 \text{ MW/km.} \quad (5-10)$$

Since a plausible efficiency of power generation in these modest temperature geothermal systems is about 15% then we estimate the average electrical power production per unit length of drilled heat exchange pipe to be $\approx 0.1 \text{ MW}_e/\text{km}$. Obviously, a lower value for the change in temperature ΔT of the rock will proportionately decrease this power estimate.

Maximum energy extraction over a period 10 years would require drilling such pipes spaced apart $2 \sqrt{\kappa_r t_r} \approx 30 \text{ m}$. Heat mining from 1 cubic kilometer of rock then requires about 1000 drilled pipes. Better estimates are possible by more detailed calculations.

The required pressure drop is not expected to be an issue for such a system since even a narrow diameter borehole may have a large fluid admittance. For example, for a 1 km pipe, the previously discussed 0.75 MW_t and $\Delta T = 100^\circ\text{C}$, the flow rate is 1.7 l/s. In a 1" diameter borehole the mean velocity is 3.4 m/s, the Reynolds number is about 3.1×10^5 , the friction factor $f = 0.038$ for an assumed surface roughness of 0.01" and the pressure drop is 90 bar/km or 9 MPa/km. The fluid admittance for a single 1 km long borehole $A = .024 \text{ l/s-bar}$ or 0.24 l/s-MPa . If indeed an array of 1000 boreholes in parallel was drilled (with a total thermal power of 750 MW_t and electrical power 100 MW_e) the admittance would be $A = 24 \text{ l/s-bar}$ or 240 l/s-MPa . These parameters are consistent with those usually discussed for EGS.

In order to understand possible design features of an engineered heat exchanger, e.g. how long such a heat exchanger should be in order to still produce a significant change in water temperature after 10 years, we give an approximate heat transfer calculation for a circular pipe of radius b . We assume the pipe has been drilled and that there is an appropriate liner to eliminate any leakage of the heat exchange fluid.

As discussed in the sections on heat transfer a one-dimensional description of the temperature change in the water is

$$v \frac{\partial T}{\partial z} = \frac{2j_r}{bC_w}, \quad (5-11)$$

where C_w is the volumetric specific heat of water and j_r is the time varying heat flux from the rock to the water. We expect that for individual pipes large enough to transport sufficient hot water for power generation the flows will be turbulent and so well mixed in the cross section, which supports this one-dimensional approximation.

Since the only mechanism of heat transfer in the rock is heat conduction we can determine the radial heat flux j_r by analyzing the heat conduction outside a cylinder of radius b . Here we just give an approximate scaling argument. We expect that on time scales such that $(\kappa_r t)^{1/2} < b$ this heat flux is controlled by the short length scale $(\kappa_r t)^{1/2}$, but as time progresses $(\kappa_r t)^{1/2} > b$ in which case the heat flux is controlled by b with (time-dependent) logarithmic corrections as a consequence of the radial geometry, i.e. approximately

$$j_r \approx \frac{k_r (T_r - T)}{b \ln \left(\frac{(\kappa_r t)^{1/2}}{b} \right)}, \quad (5-12)$$

where k_r is the thermal conductivity of the rock.

Using (5-12) we can solve the differential equation (5-11) with the boundary condition that $T(0, t) = T_w$ is the initial water temperature to obtain an estimate for the evolution of the water temperature $T(z, t)$ along the pipe:

$$\frac{T_r - T(z, t)}{T_r - T_w} = \exp \left\{ - \frac{2C_r \kappa_r z}{C_w b^2 v \ln \left(\frac{(\kappa_r t)^{1/2}}{b} \right)} \right\}. \quad (5-13)$$

Note that this expression involves the volumetric specific heat of the heat-exchange fluid and is only weakly dependent on time, which only appears explicitly in a logarithmic factor.

An engineered system will need to have drilled a length ℓ of a hole sufficient that the heat exchange remains economically viable for many years. The corresponding length of the heat exchanger is then

$$\ell \approx \frac{C_w b^2 v}{2C_r \kappa_r} \ln \left(\frac{(\kappa_r t)^{1/2}}{b} \right) \ln \left(\frac{T_r - T_w}{T_r - T(\ell, t)} \right). \quad (5-14)$$

In terms of the available thermal power P associated with the high temperature water $P \approx QC_w\Delta T$, then the length of pipe needed for the desired power is

$$\frac{\ell}{P} \approx \frac{1}{2\pi C_r \kappa_r (T(\ell, t) - T_w)} \ln \left(\frac{(\kappa_r t)^{1/2}}{b} \right) \ln \left(\frac{T_r - T_w}{T_r - T(\ell, t)} \right). \quad (5-15)$$

Again, it is important to note that this expression is only weakly dependent on time. However, this result is independent of the properties of the heat exchange fluid.

For example, suppose a reservoir has a temperature of 250° C and after 10 years of operation we still desire water temperature 150° C (where the inlet temperature is 50° C) to be produced from micro drilling a hole of diameter 1 inch or $b = 1.3 \times 10^{-2}$ m. Then, after the 10 years, in order to produce thermal power of 1 MW we would need to have drilled a pipe of length $\ell \approx 2.5$ km. This length is the order of magnitude suggested for advances in micro drilling. Furthermore, after 40 years of operation the thermal power produced would only have decreased by 10 % (or would be 0.9 MW). Based on these estimates JASON concludes that the engineered heat exchanger is a plausible idea worth further consideration.

5.3 Water

Fresh water withdrawal and consumption is an important and sensitive issue for geothermal plants operating in water-stressed areas. In addition to uses common to construction projects, geothermal systems use water when drilling wells, and to create hydraulic pressure to fracture the rock. The major water consumption, however, arises during routine operations, when water is used to cool surface heat exchangers and as feed water to replace losses from the hydrothermal reservoir. For hot dry rock or where natural hydrothermal waters become depleted, enhanced geothermal systems (EGS) also require a water supply to charge the reservoir initially. Moreover, experience has shown that natural hydrothermal systems gradually lose water

after years of operation, and even ones in “hard” rock often have channels that bleed water from the system.

Some geothermal systems, e.g. The Geysers in northern California, produce hot steam with low water content (dry steam) directly from the ground, which directly drives a turbine. The exhaust is vented to the atmosphere, although in such systems the steam can also be condensed and returned to the reservoir. When hot water comes to the surface, one approach feeds it into a tank at lower pressure, causing it to flash into steam which then can drive a turbine or heat exchanger. In one version of flash systems, the geothermal fluid heats an organic fluid in a closed loop that vaporizes at a lower temperature, drives the turbine, and returns through a condenser (Figure 5-9). Cooling water is needed for the condenser for these systems, as well as to make up water lost underground. In addition, some systems are cooled by air, known as dry cooling. This works well during cold weather but loses efficiency, sometimes by factors of two or more, in summer, when electrical demand is greatest in much of the U.S. (see also [86] and [24]).

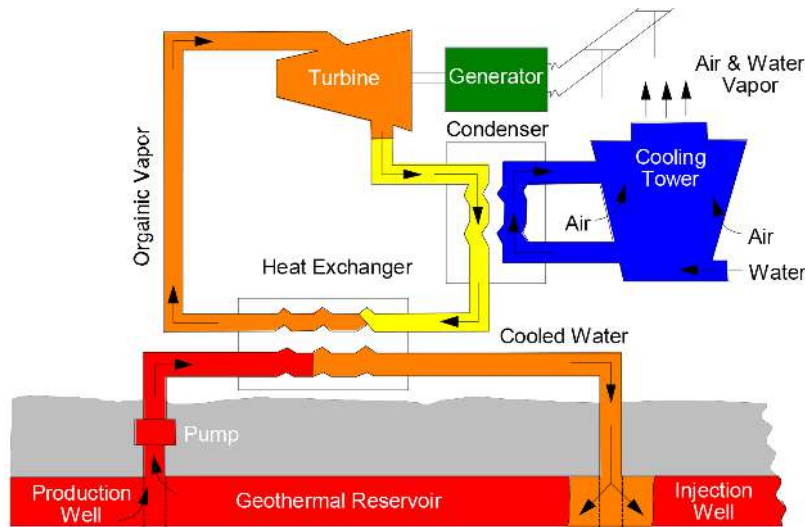


Figure 5-9: Geothermal system with binary cooling [85]. Water pumped to the surface in a production well passes through a heat exchanger and is returned to the geothermal reservoir. An organic compound that vaporizes at a temperature lower than the hydrothermal water drives a turbine and is recycled through a condenser which is cooled with water.

Estimates of water consumption demonstrate that geothermal power systems configured with a water cooling tower generally consume more water per unit of electrical energy than other power sources (Table 5.1)². This high water usage per unit energy produced is primarily due to the lower Carnot efficiency resulting from the water temperature available from the reservoir, along with subsurface losses. Nevertheless, geothermal plants are expected to implement air cooling wherever possible, which, in principle, substantially reduces water usage, perhaps to near zero. We discuss this important point next.

Not indicated above is the wide variance of water estimates that can be found for geothermal power. For example, Harto, et al. (2013) [24] take a value of 40 m³/TJ for above-ground water consumption, assuming that air cooling is used with EGS systems. Yet, as we note below, they also estimate subsurface water losses to amount to about 10³ m³/TJ for EGS, so the overall concern regarding water use – above and below-ground – is whether it amounts to 1000 or 2000 m³/TJ for EGS (see also Macknick, et al., 2011) [87].

As another example of disparate estimates, in their 2006 Geothermal Task Force report [88], the Western Governor’s Association states that a new geothermal flash plant would consume 5 gallons of fresh water per MWh compared to 361 gal/MWh for a new gas plant. The geothermal estimate is equivalent to 0.0053 m³s⁻¹/TW, compared to 10 m³s⁻¹/TW in Table 5.1 for a similar situation. The low estimate presumably assumes steam release to the atmosphere rather than cooling by air alone, and no need for reservoir recharge.

To assess the water consumption that could occur if some recharge of the geothermal recirculating fluid is needed, we consider the electrical power

²For water consumption associated with energy production, many different units are used in the literature. We convert among units according to the following: 1 gal/kWh = 10³ gal/MWh = 3.8 l/kWh = 3.8 m³/MWh = 1.05 l/MJ = 1.05 × 10³ l/GJ = 1.05 m³/GJ = 1.05 × 10³ m³/TJ

Table 5.1: Volumes of cooling water consumed per unit production of electrical energy, in units of m^3/TJ_e . The values are from engineering calculations [89], [90] except for the geothermal value which is from [91, 24]. The geothermal value applies to wet or hybrid system above-ground losses plus approximate estimates of subsurface losses.

Process	Water Consumption
Gas (CCGT)	220
Coal (steam turbine)	540
Nuclear (steam turbine)	660
Solar thermal	780
Geothermal	800-1800

for a geothermal system

$$P = \rho C_p \Delta T Q \eta \quad (5-16)$$

where ρ is the density of the water, C_p is the specific heat of the fluid at constant pressure, ΔT is the temperature drop across the heat exchanger, Q is the volume flow rate, and η is the efficiency.

We can evaluate the geothermal flow rate Q as a function of power for $\Delta T = 100$ K and 200 K, using $C_p=4200$ J kg^{-1} for the specific heat of water at constant pressure. In practice, C_p may be smaller because of its dependence on temperature and salt concentration. Geothermal water flow for a hot system, 200 K, is about 5000 $\text{m}^3 \text{s}^{-1}$ per GW and the estimate for a 100 K system is about twice that.

In an ideal case, once charged, all reservoir water would be re-used without losses. If there are losses in the system that require recharge of the recirculating fluid, the water consumption would increase, although it is possible that non-fresh water could be used. EPRI [92] estimated that with about 10% losses, consumption would increase by about 1000 m^3/TJ_e above consumption for cooling. As noted above, Harto et al. (2013) [24] give similar numbers for potential below-ground losses in the life-cycle assessments of EGS; such estimates are uncertain at the present time, however.

Water usage is of particular concern for geothermal systems because the western states of the U.S. have the highest geothermal potential, but most of the western state locations also have the lowest rainfall (Figure 5-10). Among the states, Nevada has both the highest potential and the lowest rainfall. It also has low recharge rates for its aquifers.

As a case study, in June 2013 several JASON members toured the Coso geothermal plant outside Ridgecrest, CA. A well-established natural system lying along a fault, Coso produces about 260 MW. In addition, presently about 40% of water from production wells is lost to steam. After a four-year legal fight, the plant won the right to add up to 3,000 gallons per minute ($0.19 \text{ m}^3\text{s}^{-1}$) from a well on land owned by their parent company (Andrew Sabin, personal communication). In addition, flow is watched by local Indians who are concerned about the health of their sacred fumaroles nearby.

An upper bound for water consumption at the Coso geothermal plant assumes current power production using all of the 3,000 gallons per minute ($0.19 \text{ m}^3/\text{s}$) allowed from the Hay Ranch property, yielding a value of $730 \frac{\text{m}^3}{\text{TJ}}$.

Recovering only $\approx 20\%$ of their natural steam, the Geysers found a creative solution to their water needs by using recycled (waste) water from Lakes County (9×10^6 gallons per day) and the city of Santa Rosa (12×10^6 gallons per day). The Santa Rosa project began in 1993 after the city was facing problems from discharging treated recycled water in the Russian River, and was completed in 2004, requiring 40 miles of pipes some 48 inches in diameter. The Geysers web site states that the combined recycled water consumption rate is $\approx 1 \text{ m}^3\text{s}^{-1}$. The water consumption for recharge for the ~ 700 MW facility is therefore about $1460 \text{ m}^3/\text{TJ}$. However, the use of recycled water allows this to be met without withdrawing fresh water from the local watershed.

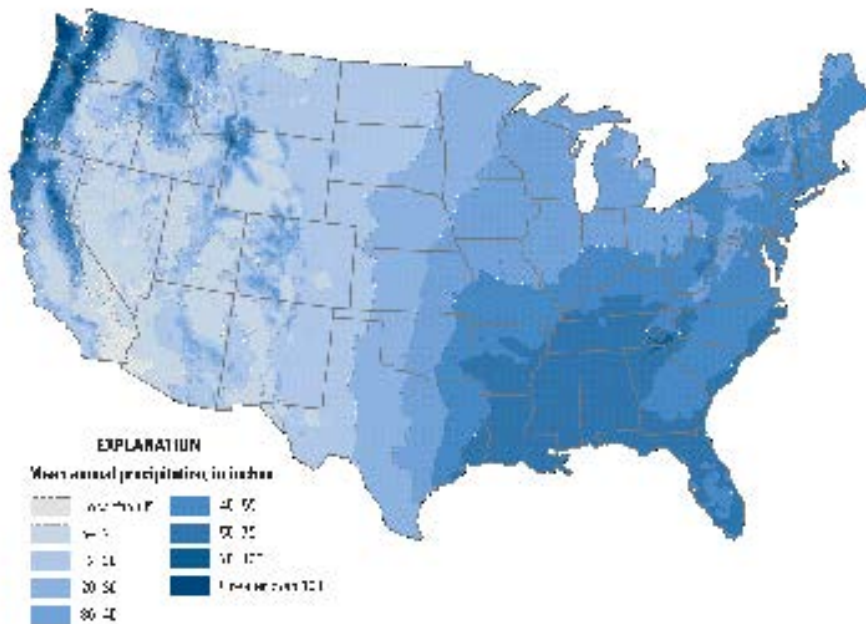
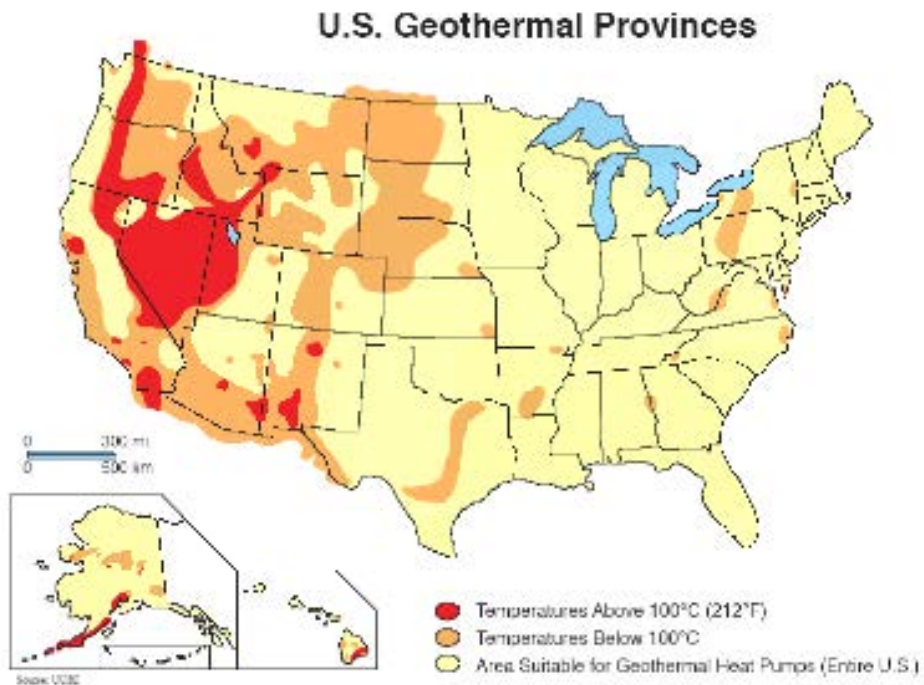


Figure 5-10: Map of U.S. Geothermal Provinces [93] (top) and annual precipitation [94] (bottom). Nevada has both the highest geothermal potential and the lowest precipitation in the U.S.

In summary, water availability can be a significant factor in operating geothermal plants in areas of water scarcity, and could become a limiting constraint for EGS at scale (see also Harto, et al., 2013 [24]).

5.4 Corrosion and Scaling

Conventional geothermal systems have significant problems with corrosion or scaling of transfer piping, and this will be an issue for EGS systems as well.

Although there is a discussion in the literature of novel possibilities using CO₂ as a heat-transfer medium, essentially all geothermal systems in operation today extract underground heat with some combination of steam and salty hot water (brine). In California, the Geysers geothermal plants in California represent one extreme, where steam carries most of the heat to the surface. The geothermal plants at the Salton Sea represent the other extreme, where much of the heat is carried by brine, which flashes to steam near the surface. High-temperature heat sources tend to be dominated by steam and lower-temperature sources by brine.

Corrosion and scaling can be caused both by gases mixed with the steam and by various substances dissolved in the brine. Much of the corrosion at the Geysers fields is caused by hydrogen chloride and hydrogen sulfide gases mixed with the steam. Brines are a mixture of dissolved substances, including dissolved CO₂, bicarbonate and carbonate ions, with relative amounts fixed by the pH of the brine, orthosilicate ions, chloride ions, sulfates or sulfides (depending on the redox state of the brine), cations of calcium, magnesium, sodium, iron, and many other metals.

Particularly troublesome is the carbonate chemistry of the brine, which can lead to intolerable scale formation, especially at high pH where bicarbonates ions which combine with ubiquitous Ca⁺⁺ ions are converted to form deposits of solid calcium carbonate, CaCO₃, usually in the form of calcite.

Precipitation conditions are hard to predict because the solubility of CaCO_3 has substantial dependence on temperature and pressure. Precipitation rates also depend on the concentration of other ions, for example Mg^{++} , which can suppress the formation of calcite in favor of aragonite, as it does in the oceans today. The use of supercritical CO_2 as a heat transfer medium is likely to exacerbate the problems of carbonate chemistry, and to introduce unanticipated new problems.

None of the chemical problems mentioned here need to be show-stoppers for EGS, but solving them will require time, funds, talent and research.

5.5 Induced Seismicity

One consequence of geothermal production is the generation of earthquakes. Induced seismicity is a relatively well-documented phenomenon associated with changing fluid pressures at depth, for instance due to impounding water behind a dam or injecting fluids into the crust, and it has on more than one occasion caused significant public concern with EGS and other geothermal projects (National Research Council, 2012; Ellsworth, 2013) [95, 96]. Small earthquakes are also caused by hydro-fracturing, as may be used for EGS stimulation, e.g., Julian et al., 2010 [97]; in fact, micro-earthquakes provide important information about the spatial distribution of stimulated zones at depth, so could have been discussed above as part of subsurface characterization (see Flewelling, et al., 2013 [98], for a recent example from the oil and gas industry).

We start, however, by noting that seismicity can be directly attributable to geothermal production, specifically to the net volume of fluid (extracted – injected volumes) in the subsurface [95, 99]. More work is needed to characterize all factors controlling seismicity associated with production, but the important point is that there is a basis for controlling the induced seismicity

and therefore for minimizing this potential hazard attributable to EGS (see also Mena, et al., 2013) [100]. Independent review has lauded DOE planning on this issue [95].

In addition, there are promising advances in understanding the stress changes associated with EGS-induced seismicity, suggesting that detailed monitoring can be used to provide quantitative monitoring at depth (e.g., Catalli, et al., 2013) [101]. This is of interest not only for reducing the hazard during production, but also as a means of characterizing subsurface volumes undergoing hydro-fracturing or other stimulation for EGS development.

Such stress measurements are complementary to the electromagnetic imaging and tracer-measurement schemes described in §4 in defining the spatial-temporal evolution of flow paths (permeability) at depth. We note the emerging sense that both the mechanical state and flow paths in the crust may typically be in a critical state, with highly nonlinear response to external forcing. For instance, small stresses (e.g., from distant earthquakes) can significantly alter flow paths or even induce rupture on critically loaded cracks (e.g., Manga, et al., 2012; Ellsworth, 2013; van der Elst, et al., 2013; Wang, et al., 2013) [96], [102] – [105].

Microseismicity (numbers and locations of events) can be monitored over thousands of meters, but we advocate more detailed measurements coupling estimates of spatio-temporally varying permeability and stress-state based on coupling tracer and electromagnetic with seismic methods. In order to further develop and validate these approaches at field-scale, initial studies could be applied across short distances (e.g, tens of meters), possibly using the micro drilling ideas discussed in Section 4.7 before moving to the more practical scales relevant to EGS stimulation and production monitoring (hundreds of meters or more).

References

- [1] N. E. Todreas and M. S. Kazimi, *Nuclear Systems I: Thermal Hydraulic Fundamentals*, Taylor and Francis, New York, 720 pp (1989).
- [2] Reimus, P., *et al. Thirty-Seventh Workshop on Geothermal Reservoir Engineering* (Stanford U., Stanford, Cal. 2012) SGP-TR-194.
- [3] Rose, P., *et al. Thirty-Seventh Workshop on Geothermal Reservoir Engineering* (Stanford U., Stanford, Cal. 2012) SGP-TR-194.
- [4] Reimus, P. email to J. Katz July 24, 2013.
- [5] Rose, P. email to J. Katz July 25, 2013.
- [6] Rose, P. E. and Adams, M. C. *Geothermal Resources Council TRANSACTIONS* **18**, 237–240 (1994).
- [7] Fine, R. A. and Millero, F. J. *J. Chem. Phys.* **59**, 5529 (1973).
- [8] Jung, R. *EGS — Goodbye or Back to the Future*, Chap. 5 pp. 95–121 <http://dx.doi.org/10.5772/56458> (2013).
- [9] Grant, M. A. and Garg, S. K. *Thirty-Seventh Workshop on Geothermal Reservoir Engineering* (Stanford U., Stanford, Cal. 2012) SGP-TR-194.